Robust Adaptive Waveform Inversion

Mike Warner, Imperial College London & Lluís Guasch, Sub Salt Solutions Limited*

Summary

Adaptive Waveform Inversion (AWI) was introduced by Warner & Guasch (2014) as a means to avoid cycle skipping during full-waveform inversion. Here we demonstrate the robustness of this new method by applying it to three challenging problems: a 3D field dataset without an accurate velocity model to start the inversion; a highly realistic blind synthetic dataset that contains elastic effects, attenuation, an unknown density model and ambient noise; and a simple synthetic dataset where the inversion proceeds using the wrong source wavelet. AWI outperforms conventional FWI in each of these applications, and remains stable and accurate throughout.

Introduction

Conventional full-waveform inversion minimizes the least-squares difference between an observed and a predicted dataset. Because seismic data are oscillatory, this formulation leads to an objective function that is also oscillatory, generating local minima that represent cycle-skipped solutions where the predicted and observed datasets differ by an integer number of cycles. This behavior is the principal reason why FWI requires low frequencies and a highly accurate starting model.

In contrast, adaptive waveform inversion uses convolutional filters to match predicted and observed data, and the inversion is formulated so that it forces the resultant filter coefficients to become zero-lag delta functions. The resulting AWI scheme appears to be entirely immune to the effects of cycle skipping.

AWI has several additional supplementary benefits that also make it superior to conventional FWI. AWI is more able to extract long-wavelength velocity updates from reflection data than is FWI. Surprisingly, AWI also revealed for the field dataset used here that a previous starting model, obtained using high-quality anisotropic travel-time tomography, was cycle skipped for parts of the dataset even at the lowest frequencies available for inversion. This hitherto unsuspected cycle skipping caused detrimental artifacts within the original conventional FWI model, and AWI successfully removed these artifacts.

AWI is one of a family of methods that work by extending the size of the model space in non-physical ways, and that then seek to drive such non-physicality out of the final recovered model. Conventional wave-equation migration velocity analysis proceeds by following an analogous route.

Theory

Conventional FWI seeks to minimize the least-squares objective function f given by

$$f = \| \mathbf{p(m)} - \mathbf{d} \|^2$$

where the column vector **d** represents the field data, and **p** represents the equivalent data predicted by a model **m**. In contrast, AWI employs convolutional filters to match the two datasets, performing the inversion conceptually in two stages. The first stage is to design a Wiener filter **w**, that matches a predicted trace **p** to an observed trace **d** by minimizing the least-squares objective function f_1 given by

$$f_1 = \| \mathbf{Pw} - \mathbf{d} \|^2$$

where **P** is a matrix representation of convolution by the vector **p**. Then, in a second stage, we minimize a normalized least-squares objective function f_2, given by

$$f_2 = \frac{\| \mathbf{Tw} \|^2}{\| \mathbf{w} \|^2}$$

where **T** is a simple diagonal matrix that acts to weight the filter coefficients as a monotonic function of the magnitude of the temporal lag. Minimizing f_2 with respect to the model **m** pushes the predicted data **p** towards the observed data **d**, and so pushes the model **m** towards the true model. The objective functions f_1 and f_2 are not oscillatory and do not suffer from the detrimental effects of cycle skipping.

There are several ways to understand how AWI operates. One of the simplest is to realize that, in order to match a single predicted to a single observed trace for one source and one receiver, there are two ways that we might proceed. One is the change the sub-surface model, but the other is to change the source wavelet. Provided that we are able to employ a wavelet that is infinitely long and acausal, then this second strategy will always be possible. AWI adopts this second strategy, using Wiener filters as least squares approximations to the required infinite wavelets.

Initially, every trace in the dataset requires a different source wavelet. The AWI functional f_2 is designed to alter the model **m** so that it drives all these wavelets towards the actual wavelet that was used to acquire the original data. Once this is achieved, the model will fit the observed data using the correct source. In practice, AWI works optimally when it is configured to match an observed to a predicted trace; that is, we actually use the inverse of **w** in f_2.

DOI http://dx.doi.org/10.1190/segam2015-5853026.1

Results – problem one

Figure 1 shows the results of applying both conventional FWI and AWI to a 3D field dataset. Results on the left begin from a high-quality starting model obtained by a major contractor using anisotropic travel-time tomography, while those on the right begin from a simple one-dimensional starting velocity model obtained from time-migrated gathers. The first row shows the starting model, the second row shows the FWI-recovered model, and the final row shows the AWI-recovered model. Columns one and three are at 1200 m depth, and columns two and four are at 2100 m depth. The feature near the centre is a low-velocity gas cloud. The data were inverted in the time domain in the range 3 – 7 Hz. For the good starting model, we used six iterations per source; for the bad starting model we used twice the total number of iterations; the number of iterations necessary appears to increase as the starting model becomes further from the true model.

Using the good starting model, the results obtained by both FWI and AWI are similar, especially around the gas cloud. However the models differ in the bottom left of the figures, where low-velocity (green) artefacts appear in the FWI result. Further investigation revealed that these artefacts were produced by previously unsuspected cycle skipping of late refracted phases at the longest offsets in this portion of the model, and the FWI results are consequently incorrect.

Using the poor starting model, the contrast between the FWI and AWI results is more marked. The FWI result is now severely cycle skipped at the longest offsets, and this compromises the recovery of the gas cloud and introduces significant spurious structure. In contrast, the AWI result is largely unaffected by the quality of the starting model; cycle skipping is not apparent in the results. However, since the inversion begins further from the true result, the total number of iterations required increases, and AWI has not yet fully converged for the deeper section.

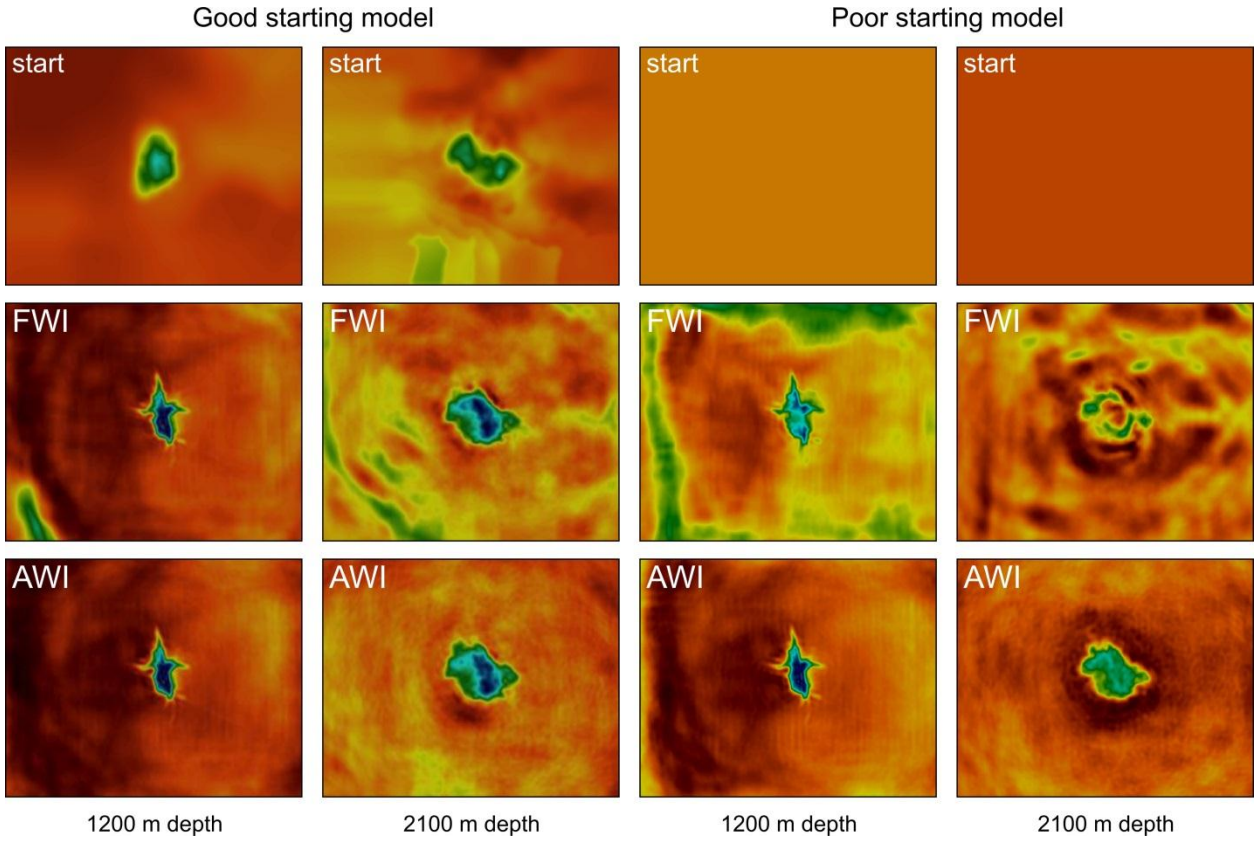

Figure 1: FWI and AWI inversion results from a 3D field dataset in shallow water. Horizontal slices show p-wave velocity at depths of 1200 and 2100 m. Images on the left use an accurate starting model, those on the right use a simple 1D starting model.

DOI http://dx.doi.org/10.1190/segam2015-5853026.1

Results – problem 2

In 2014, Chevron designed a highly realistic seismic model, based upon field seismic data, well logs and rock physics. Using this model, they generated fully visco-elastic synthetic data, simulating a conventional 2D towed-streamer marine acquisition geometry with a maximum offset of 8000 m. The model has a non-deterministic, realistic relationship between velocity and density, it is locally isotropic, it has limited bandwidth, ambient noise, surface ghosts and surface multiples, and is modelled using the full visco-elastic two-way wave equation.

Figure 2(a) shows the starting model. This has the true bathymetry, but is otherwise one dimensional. It was not obtained by smoothing the true model. For the offsets available in the seismic data, useful refracted energy does not penetrate the model below about 2 km depth. Figure 2(b) shows the result of applying conventional FWI to these data, starting at 3 Hz, and increasing the bandwidth by stages to 10 Hz.

The FWI result is cycle skipped at both ends of the model. FWI produces useful and sensible velocity updates over the top 2 km of the model where it is not cycle skipped, but it produces only minor updates below the region that is penetrated by refractions. FWI produces no significant long-wavelength update below about 2 km, and it does not migrate deeper reflectivity structure accurately into the model because the long-wavelengths are not yet correct.

Figure 2(c) shows the final result of applying AWI, from 3 to 10 Hz, successively in three stages, followed by conventional FWI applied from 10 to 27 Hz. Both reflections and refractions were retained throughout, and multiples, ghosts and other non-primary phases were included. Using AWI, the cycle skipping is overcome, and significant long-wavelength macro-velocity updates are now obtained from pure reflection data, especially in the major low-velocity layer around 2.5 km depth. In contrast, conventional FWI can only recover the model correctly in this region if the starting model is first independently improved to obtain the correct long-wavelength behaviour.

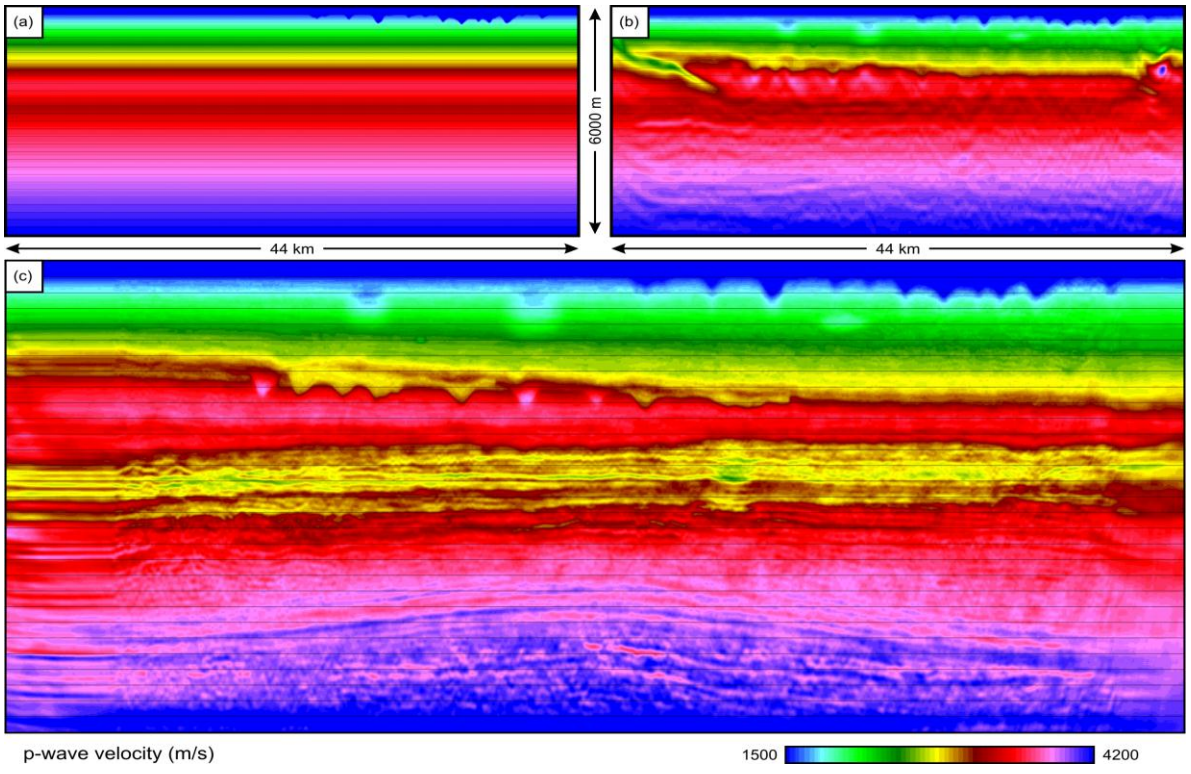

Figure 2: (a) Start model, (b) FWI recovered model showing cycle skipping and limited recovery below 2 km, (c) Model recovered by AWI followed by FWI; there is no cycle skipping and good recovery from pure reflection data below 2 km depth.

DOI http://dx.doi.org/10.1190/segam2015-5853026.1

Results – problem 3

Figure 3 shows results from a portion of the well-studied Marmousi model. Here we show the results of inverting synthetic data using both a correct and an incorrect source wavelet – as shown by the inset. Both sources have approximately the same bandwidth, and their nominal zero times and polarities are the same.

Figures 3a and 3c show FWI and AWI applied using the correct source. Both recovered models are similar since there is no cycle skipping in this problem, and there is good refraction coverage over most of the model. Figures 3b and 3d show the equivalent results produced when the inversion proceeds using an incorrect source. As would be expected, this degrades both results, but AWI is clearly much more robust to this erroneous assumption than is FWI – Figure 3d gives a much better result than that shown in Figure 3b.

Summary & Conclusions

AWI is able to overcome cycle skipping in both synthetic and field data. It is able to extract more information about the long-wavelength velocity model from pure reflection data than is conventional FWI. AWI is robust in the presence of elastic effects, attenuation, multiples and ambient noise, and is less sensitive to errors in the assumed source wavelet than is FWI. AWI works well in combination with FWI; beginning with the former and ending with the latter is able to provide the benefits of both.

Acknowledgements

AWI and Adaptive Waveform Inversion are trademarks of Sub Salt Solutions Limited. AWI is the subject of GB patent 25092234. We thank Chevron for generating a realistic and challenging dataset for problem two.

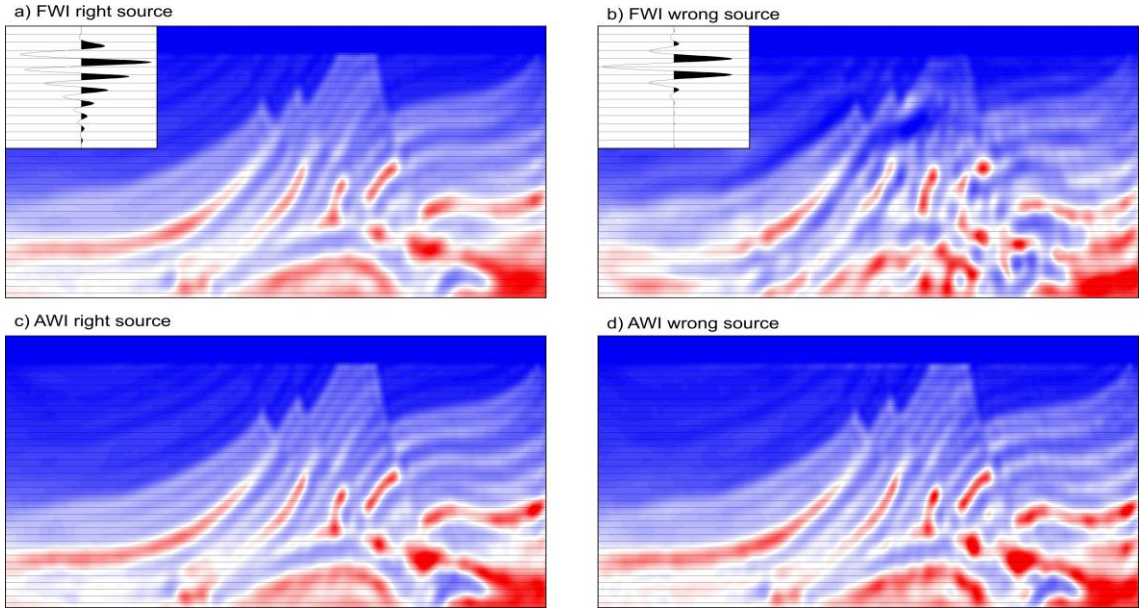

Figure 3: Inversions of the Marmousi model using both FWI and AWI from a non-cycle skipped starting model. The results on the left assume the same source for the inversion as was used to generate the synthetic data, while results on the right assume the wrong source. The actual wavelets used in both cases are shown by the insets. AWI is robust to errors in the source estimation while FWI is much less robust.

DOI http://dx.doi.org/10.1190/segam2015-5853026.1

EDITED REFERENCES

Note: This reference list is a copyedited version of the reference list submitted by the author. Reference lists for the 2015 SEG Technical Program Expanded Abstracts have been copyedited so that references provided with the online metadata for each paper will achieve a high degree of linking to cited sources that appear on the Web.

REFERENCES

Warner, M., and L. Guasch, 2014, Adaptive waveform inversion: FWI without cycle skipping: 76th Conference & Exhibition, EAGE, Extended Abstracts, doi:10.3997/2214-4609.20141093.